21st Australasian Fluid Mechanics Conference
Adelaide, Australia
10-13 December 2018

Shallow Water Island Wakes in Unsteady Tidal Flows

P. M. Branson[1], M. Ghisalberti[1,2] and G. N. Ivey[1]

[1]Ocean Graduate School
University of Western Australia, Crawley, Western Australia 6009, Australia

[2]Department of Infrastructure Engineering
University of Melbourne, Parkville, Victoria 3010, Australia

Abstract

Islands have been observed to play a key role in the vertical and cross-shelf mixing processes occurring in topographically-complex regions with strong tidal forcing. Satellite observations of suspended solids and temperature have confirmed the capacity of islands to mix the water column over the depth and deliver nutrient-rich deeper water into the photic zone. The stability of the island wake establishes the wake form, which in turn controls the spatial and temporal distribution of mixing zones. Therefore it is important to understand the physical processes that govern island wake stability. To date, shallow water island wake dynamics, stability and the transition to vortex shedding has predominantly been investigated for steady flows, this study investigates shallow water island wake structure for the more general case of unsteady tidal flow.

A laboratory study of shallow islands with circular cross section subjected to unsteady tidal forcing has been undertaken in the Shallow Tidal Flow Flume at UWA. Three-dimensional particle imaging velocimetry has been applied to synthetic aperture images of the near island flow to resolve the evolution of the wake horizontal velocity profile and vertical structure. The spatial and temporal evolution of a vortex shedding wake and unsteady bubble wake are examined through parametric fitting of an analytical wake velocity profile. It is demonstrated that increasing wake stability, through an increasing relative influence of bed friction, modifies the wake through three key mechanisms: 1) attenuating the return flow in the wake during the accelerating stage of the tide 2) damping the growth of the vortex shedding instability and 3) establishing a return flow jet during the decelerating phase. The return flow jet of the unsteady bubble wake subsequently establishes a stronger separation shear layer extending from the flank of the island during the early stages of the subsequent acceleration stage. This highlights a fundamental link between the wake evolution and flow separation at the island flanks.

Introduction

The spatial distribution of upwelling depends on the development and evolution of primary vortices (with a vertical axis of rotation) and their associated secondary vortices (those with a horizontal axis of rotation). The three dimensional spatial distribution of these flow structures play an important role in the spatial distribution of upwelling and downwelling [5]. Numerous field studies have noted the importance of the complex flow features associated with island wakes for aggregating sediments and plankton [17, 11, 15], which may influence the distribution of benthic and higher order pelagic organisms [16, 12, 13]. Improved understanding of the physical processes that govern wake stability is necessary to better predict the role that islands play in mixing on continental shelves.

Studies of shallow water island wakes have predominantly investigated the evolution of the wake in a steady external flow [8, 17, 6]. However, more generally on continental shelves subjected to tidal forcing the external flow is unsteady. The time scale of flow unsteadiness establishes a vertical structure in horizontal velocity that is dependant on the relative thickness of the boundary layer compared to the flow depth $\delta^+ \sim \sqrt{\nu T}/h$ where h is the flow depth and ν the kinematic viscosity and T is the tidal period [5]. The vertical structure of the flow field has been demonstrated to play a key role in the growth of instability both within shallow vortices [9] and shallow island wakes [5]. When the tidal excursion is long compared to the island diameter, as quantified by the Keulegan-Carpenter number $KC \sim U_0 T/D$ (where U_0 is the amplitude of the sinusoidally varying tidal velocity, and D is the island diameter), two archetypal wake forms have been observed: 1) the vortex shedding wake and 2) the unsteady bubble wake [5].

In steady shallow wake flow, the stability parameter, $S_s = c_f D/h$ where c_f is a friction coefficient, predicts well the transition from the unsteady bubble wake to vortex shedding with vortex shedding commencing for $S_s \lesssim 0.2$ [6, 10]. From the analytical solution of the laminar, oscillatory boundary layer it can be shown that $c_f = 1/ka$, where $k = \sqrt{\Omega/2\nu}$ is the wave number of the oscillatory boundary layer and $a = U_0/\Omega$ the fluid excursion above the boundary layer (with $\Omega = 2\pi/T$) [1]. Utilising this definition of c_f, the wake stability parameter for tidal flow around islands is $S = \sqrt{4\pi}\frac{\delta^+}{KC}$ [3].

This paper presents the preliminary results of a laboratory study of island wake stability for idealised islands with circular cross section. This study is the first examination of the spatial and temporal evolution of the unsteady shallow wake through the parametric fit of an analytical function typically utilised in stability analysis of the lateral profile of streamwise velocity.

Methods

Experimental setup

Experiments were conducted in the Shallow Tidal Flow Flume in the Geophysical Fluid Dynamics laboratory at the University of Western Australia. The flume had a working section 185 cm wide, 600 cm long and up to 35 cm deep. The flume was recirculating and used a software controlled (NI LabView) variable frequency drive and pump able to generate a reciprocating tidal flow with a near sinusoidal horizontal velocity signal. Polycarbonate flow straighteners were utilised in each end of the flume to produce a near uniform transverse velocity profile. The experimental flow conditions are detailed in table 1. Each flow was established for 10 cycles, before being sampled for 8 cycles. An array of 9 cameras were used to obtain three dimension and three component velocity measurements via three dimensional particle imaging velocimetry applied to synthetic aperture images [2]. Further details of the experimental setup, PIV algorithm, measurement validation and error are presented in [5, 4]. The error in the instantaneous velocity measurements for these experiments was estimated as up to 5-10% [4].

Table 1: Conditions of the experimental runs, $KC = U_0 T/D$, $\delta^+ = \sqrt{\nu T}/h$, $Re_D = U_0 D/\nu$ and $S = \sqrt{4\pi}\frac{\delta^+}{KC}$.

Wake type	U_0 [cm s^{-1}]	T [s]	h [cm]	δ^+	KC	Re_D	h/D	S
Unsteady Bubble	2.80	85.9	2.3	0.40	24.1	2805	0.23	0.06
Vortex shedding	4.44	60.0	5.3	0.15	26.7	4446	0.53	0.02

In this study x, y and z are the streamwise (u), cross-stream (v) and vertical (w) directions respectively. The origin is defined at the bed level in the centre of the island. The peak tidal velocity U_0 is estimated from the amplitude of the sinusoidally varying velocity at the top of the boundary layer $z_{BL} = \frac{3\sqrt{\pi}}{4}\delta^+$ [1]. To phase-align the results, the time $t = 0$ is defined at the u zero-crossing at height z_{BL}. Thus, the phase of each experimental condition is defined as $\phi = t/T \mod 1$. The camera array is observing the downstream wake for $0.5 < \phi < 1.0$, with $0.5 < \phi < 0.75$ the accelerating stage of the tidal cycle and $0.75 < \phi < 1.0$ the decelerating stage. The velocity data is phase averaged over 8 cycles, with the phase average (of, for example, the streamwise velocity) denoted by $\tilde{u}$.

Parametric Fitting to Analytical Wake Profile

Previous investigations of both unbounded and shallow water cylinder wakes have demonstrated that a hyperbolic sinusoidal profile represents the lateral (cross stream) profile of streamwise velocity in the wake, and for this reason it has been utilised extensively in stability analysis [14, 7]. The general form of the normalised streamwise velocity wake profile in the lateral y direction is given by [14]:

$$\overline{u}(\hat{y}) = 1 - R + \frac{2R}{1 + \sinh(\hat{y}/l)^{2N}} \tag{1}$$

where $R = (U_c - U_m)/(U_c + U_m)$ is the velocity ratio with U_c the minimum velocity and U_m the velocity outside the wake, N is the "shape parameter", l is the transverse length scale and $\hat{y} = y/D$. For $R = -1$ the wake has zero minimum velocity, while for $R < -1$ a reverse flow (towards the island) is present. The shape parameter N controls the ratio of the mixing layer thickness to the wake width [14]. In the steady shallow wake R gradually increases downstream due to entrainment into the wake and damping due to bed friction [7]. N decreases downstream as the mixing layer thickness grows with an asymptote of $N = 1$.

The time-averaged streamwise velocity profile ($\overline{u}(y)$) in a wake with a steady external flow is symmetric about the wake centreline with a minimum velocity occurring on the wake centreline. In contrast for island wakes in tidal flow, the depth and phase averaged streamwise velocity profile ($\tilde{u}(y,\phi)$) may be asymmetric, with the minimum velocity (U_c) not necessarily occurring along the wake centreline and the velocity outside the wake not necessarily equal on each flank. To allow for wake asymmetry the wake profile is fitted to each flank independently. Prior to calculating the profile fit, U_c and U_m are determined for each flank independently based on the measured data. We define $\hat{y} = 0$ where $u = U_c$ and U_m as the maximum streamwise velocity on the given flank. For each flank the data utilised for the fit is extended by $y/D = 0.25$ past the location of U_c (towards the opposite flank) to improve the fit for the shape of the wake centre. A non-linear least squares algorithm is applied to obtain the parameter estimates for R, N and l.

Results

An example of two different wake forms is presented in figure 1. Whilst both flow conditions have similar KC, the larger value of δ^+ enhances the wake stability, suppressing vortex shedding and altering the spatial distribution of up- and downwelling flow structures. This in turn is expected to alter regions of productivity and tracer aggregations associated with these different wake forms, with subsequent ecological implications.

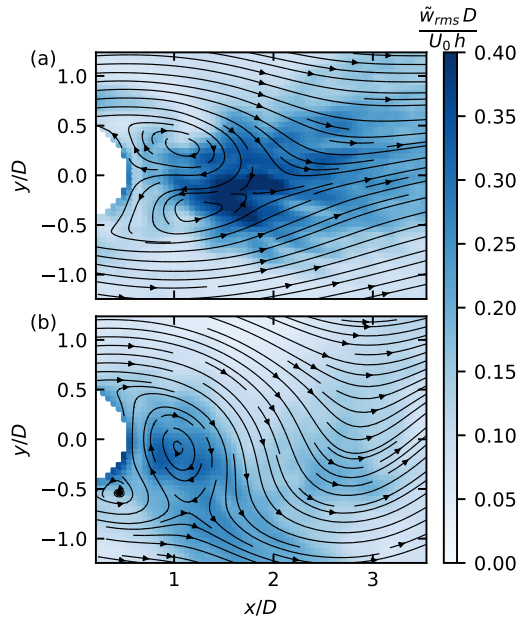

Figure 1: Comparison of the phase and depth averaged flow field at $\phi = 0.875$ in the (a) unsteady bubble and (b) vortex shedding wakes with the horizontal flow field shown by stream lines. The colour indicates the phase-averaged normalised root-mean-square vertical velocity at $\phi = 0.875$. The spatial distribution of up- and downwelling is strongly influenced by the wake form.

Beginning of Tidal Acceleration

Wake velocity profile fits have been performed at three different locations and at three different phases to highlight some of the key changes that occur in the lateral profile of velocity with increasing wake stability. Wake stability analysis for steady external flow has demonstrated that the value of R strongly influences the overall wake stability. As the unsteady wake develops both in time and space we contrast the unsteady bubble and vortex shedding wake profiles for increasing ϕ at increasing distance downstream where R is at a minimum.

At the beginning of the tidal acceleration stage ($\phi = 0.6$), close to the island ($x/D = 0.6$), the unsteady bubble wake has a jet that extends from the flow separation point, as demonstrated by the large velocity overshoot (figure 2, upper left panel). The analytical profile utilised does not describe this jet, and whilst the fitted profile follows the shear layer adjacent to the island reasonably, it overestimates R somewhat. The jet creates a strong shear layer on both flanks of the island, as indicated by $N > 2$. The vortex shedding wake does not exhibit a tidal jet and

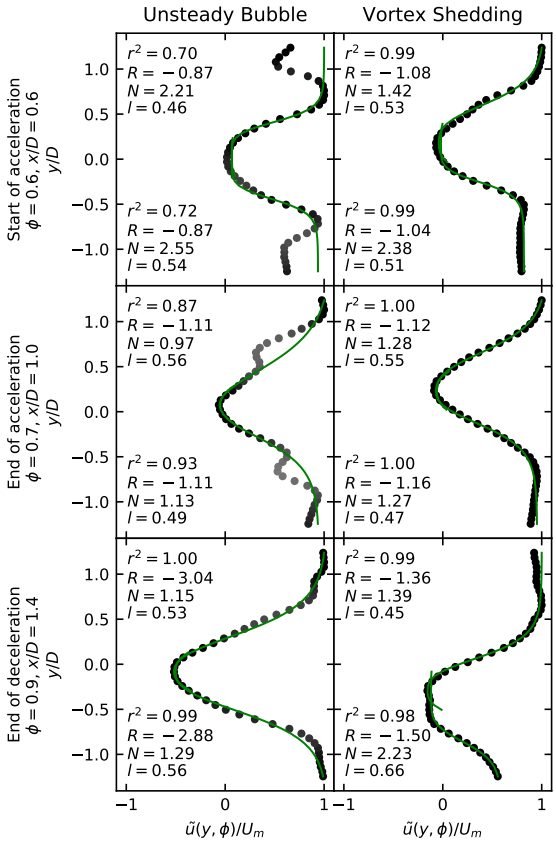

Figure 2: Scatter plot of phase and depth averaged streamwise velocity at key stages of the tide and locations downstream of the island for the (left column) unsteady bubble wake and (right column) vortex shedding wake. The parameteric profile fit is shown in green with coefficient of determination (r^2) and profile parameters inset. Top row: Start of the acceleration stage ($\phi = 0.6$) close the island ($x/D = 0.6$). Middle row: End of the acceleration stage ($\phi = 0.7$) half an island diameter downstream ($x/D = 1.0$). Bottom row: End of the deceleration stage ($\phi = 0.9$) 0.9 island diameters downstream ($x/D = 1.4$).

demonstrates significant asymmetry in the strength of the shear layers with the lower shear layer having a much larger N (figure 2, upper right panel). The profile fit is quite good for both flanks and a negative return flow ($R < -1$) is present at this early stage of the tidal flow.

End of Tidal Acceleration

By the end of the tidal acceleration stage, $\phi = 0.7$ (close to the peak in horizontal velocity) at $x/D = 1.0$ the unsteady bubble wake has developed a small return velocity and the mixing layer thickness has grown to approximately $0.5D$ (figure 2 middle left). The lighter grey points are velocity measurements that are attenuated due to aggregations of particles on the bed around $y/D \approx \pm 0.75$. The grey-scale indicates the relative weighting of the points in the non-linear fitting process, further details of how the weight is calculated is provided in [4]. The presence of such particle aggregates in this zone of convergence highlights that wake secondary circulations influence the distribution of tracers within the flow. The vortex shedding wake has developed a similar strength return flow to the unsteady bubble, but with a smaller relative mixing layer thickness, indicated by $N \approx 1.3$. The vortex shedding wake also exhibits a peak return flow that is offset from the island centreline due to the vortex shedding process.

End of Tidal Deceleration

As the tide proceeds into the deceleration phase, the adverse pressure gradient (acting to decelerate the external flow) significantly alters the evolution of the wake. In contrast to steady wake flow, where a minimum return velocity ratio of $R = -2.07$ was observed for both the unsteady bubble wake and vortex shedding wakes [6], by the end of the deceleration phase the unsteady bubble wake has obtained a minimum $R \approx -3.0$. It is this strong return flow that establishes the tidal jet that is present in the unsteady bubble wake at the beginning of the acceleration stage. By contrast the vortex shedding wake has significant asymmetry with the flow deceleration leading on the lower flank.

Spatial and Temporal Evolution of the Shallow Island Wake

Early in the acceleration stage the vortex shedding wake establishes a return flow that is not present in the unsteady bubble wake (figure 3a). The presence of a return flow has been identified as a key process leading to instability and vortex shedding [7]. The spatial decay of the velocity deficit in the acceleration stage occurs over the same distance in both the wake types. By the end of the acceleration stage, both wakes have developed a reasonably consistent structure with a minimum velocity ratio of $R \approx -1.3$ (figure 3b). As the deceleration stage commences, both the unsteady bubble wake and vortex shedding wake exhibit a reduction in R to -1.5 (figure 3c). In the unsteady bubble wake the minima in R shifts downstream throughout the deceleration stage, reaching $R \approx -3.0$ by the end of the deceleration stage (figure 3d). This is in stark contrast to the shallow, steady island wake where increasing friction reduces the downstream extent of the return flow region.

The relative mixing layer thickness, N, is highly variable initially in the acceleration stage (figure 3e), however by the end of the acceleration stage exhibits a rapid increase in thickness (decreasing N) by $x/D = 1.0$ with an asymptote of $N \approx 1.25$ (figure 3f). This feature is present throughout the remainder of the tidal cycle (figure 3g-h). Previous studies of shallow, steady wake flow have utilised $N = 1.0$ [7], suggesting that the relative mixing layer thickness is somewhat thinner in unsteady flow compared to steady flow.

The transverse length scale parameter, l, is highly variable at $\phi = 0.6$, however exhibits a general increase with distance downstream (figure 3i). By the end of the acceleration stage the unsteady bubble wake exhibits a decreasing transverse length scale with distance downstream whereas the vortex shedding wake exhibits an increasing transverse length scale (figure 3j). As the tide progresses through the deceleration stage the transverse length scale of the unsteady bubble wake widens on both flanks as the reverse flow jet develops (figure 3k-i).

Conclusions

This study demonstrates that the hyperbolic sinusoidal profile (equation 1) can represent the lateral (cross stream) profile of streamwise velocity in shallow, unsteady island wake flow reasonably well. The lateral position of the profile must be shifted to account for the phase variation of the position of the minimum streamwise velocity and each flank of the wake fitted separately to allow for asymmetry in the external flow velocity. The vortex shedding and unsteady bubble island wakes were contrasted through comparison of the wake profile parameters in space and time and reveal important differences between shallow island wake flow subjected to tidal flow compared to steady flow.

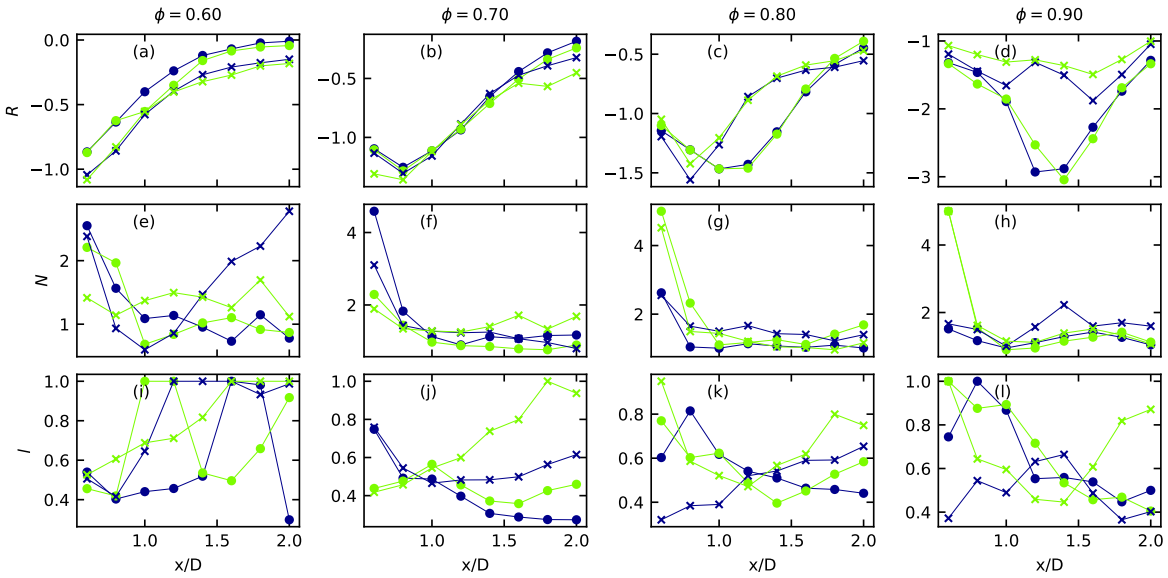

Figure 3: Scatter plots of wake profile parameter variation downstream (increasing x/D) through the acceleration ($\phi = 0.6$ and $\phi = 0.7$) and deceleration ($\phi = 0.8$ and $\phi = 0.9$) stages of the tide. Vortex shedding wake ($\times$) and unsteady bubble wake ($\bullet$) parameters. Fit parameters for the upper flank of the island are shown in light green and the lower flank in dark blue. Top row: R velocity ratio. Middle row: N relative mixing layer thickness. Bottom row: l transverse length scale.

Acknowledgements

This work was supported by resources provided by the Pawsey Supercomputing Centre with funding from the Australian Government and the Government of Western Australia.

References

[1] Batchelor, G., *An introduction to fluid dynamics*, Cambridge mathematical library, Cambridge University Press, 1967.

[2] Belden, J., Truscott, T. T., Axiak, M. C. and Techet, A. H., Three-dimensional synthetic aperture particle image velocimetry, *Meas. Sci. Technol.*, **21**, 2010, 125403.

[3] Branson, P., Ghisalberi, M., Ivey, G. and Hopfinger, E., Scaling of upwelling and secondary circulation in shallow island wakes, *J. Fluid Mech.*, **to appear**.

[4] Branson, P. M., *Shallow island wake stability and upwelling in tidal flow measured by 3D particle imaging velocimetry*, Ph.D. thesis, Ocean Graduate School, University of Western Australia, 2018.

[5] Branson, P. M., Ghisalberti, M. and Ivey, G. N., Three-dimensionality of shallow island wakes (to appear), *Journal of Environmental Fluid Mechanics*.

[6] Chen, D. and Jirka, G. H., Experimental study of plane turbulent wakes in a shallow water layer, *Fluid Dyn. Res.*, **16**, 1995, 11 – 41.

[7] Chen, D. and Jirka, G. H., Absolute and convective instabilities of plane turbulent wakes in a shallow water layer, *J. Fluid Mech.*, **338**, 1997, 157–172.

[8] Chu, V., Wu, J. and Khayat, R., Stability of turbulent shear flows in shallow channel, in *Proceeding of the 20th Congress of IAHR, Moscow*, 1983, volume 3, 128–133, 128–133.

[9] Duran-Matute, M., Kamp, L. P. J., Trieling, R. R. and van Heijst, G. J. F., Regimes of two-dimensionality of decaying shallow axisymmetric swirl flows with background rotation, *J. Fluid Mech.*, **691**, 2012, 214.

[10] Grubišić, V., Smith, R. B. and Schär, C., The effect of bottom friction on shallow-water flow past an isolated obstacle, *J. Atmos. Sci.*, **52**, 1995, 1985–2005.

[11] Ingram, R. G. and Chu, V. H., Flow around islands in rupert bay: An investigation of the bottom friction effect, *J. Geophys. Res.*, **92**, 1987, 14521–14533.

[12] Jenner, K., Jenner, M. and McCabe, K., Geographical and temporal movements of humpback whales in western australian waters, *APPEA Journal*, **38**, 2001, 692–707.

[13] Johnston, D. W. and Read, A. J., Flow-field observations of a tidally driven island wake used by marine mammals in the bay of fundy, canada, *Fish. Oceanogr.*, **16**, 2007, 422–435.

[14] Monkewitz, P., The absolute and convective nature of instability in two-dimensional wakes at low reynolds numbers, *Phys. Fluids*, **31**, 1988, 999.

[15] Pattiaratchi, C., James, A. and Collins, M., Island wakes and headland eddies: a comparison between remotely sensed data and laboratory experiments, *J. Geophys. Res.*, **92**, 1987, 783–794.

[16] Wolanski, E. and Hamner, W., Topographically controlled fronts in the ocean and their biological influence., *Science (New York, NY)*, **241**, 1988, 177.

[17] Wolanski, E., Imberger, J. and Heron, M. L., Island wakes in shallow coastal waters, *J. Geophys. Res.*, **89**, 1984, 10553–10569.